



HAL
open science

An asymptotic-numerical method to compute the postbuckling behaviour of elastic plates and shells

Lahcen Azrar, Bruno Cochelin, Nouredine Damil, Michel Potier-Ferry

► To cite this version:

Lahcen Azrar, Bruno Cochelin, Nouredine Damil, Michel Potier-Ferry. An asymptotic-numerical method to compute the postbuckling behaviour of elastic plates and shells. *International Journal for Numerical Methods in Engineering*, 2005, 36 (8), pp.1251-1277. 10.1002/nme.1620360802. hal-04785875

HAL Id: hal-04785875

<https://hal.science/hal-04785875v1>

Submitted on 15 Nov 2024

HAL is a multi-disciplinary open access archive for the deposit and dissemination of scientific research documents, whether they are published or not. The documents may come from teaching and research institutions in France or abroad, or from public or private research centers.

L'archive ouverte pluridisciplinaire **HAL**, est destinée au dépôt et à la diffusion de documents scientifiques de niveau recherche, publiés ou non, émanant des établissements d'enseignement et de recherche français ou étrangers, des laboratoires publics ou privés.



Distributed under a Creative Commons Attribution - NonCommercial 4.0 International License

AN ASYMPTOTIC-NUMERICAL METHOD TO COMPUTE THE POSTBUCKLING BEHAVIOUR OF ELASTIC PLATES AND SHELLS

L. AZRAR, B. COCHELIN, N. DAMIL* AND M. POTIER-FERRY

Laboratoire de Physique et Mécanique des Matériaux, URA CNRS 1215, Institut Supérieur de Génie Mécanique et Productique, Université de Metz, Ile du Saulcy, 57045 Metz Cedex, France

SUMMARY

In this paper, we apply an asymptotic-numerical method for computing the postbuckling behaviour of plate and shell structures. The bifurcating branch is sought in the form of polynomial expansions, and it is determined by solving numerically (FEM) several linear problems with a single stiffness matrix. A large number of terms of the series can easily be computed by using recurrent formulas. In comparison with a more classical step-by-step procedure, the method is rapid and automatic. However, the polynomial expansions have a radius of convergence which limits the validity of the solution to a neighbourhood of the bifurcation point. In the present form, the method should be viewed as a cheap and automatic way of completing a linear buckling analysis. It is illustrated in two examples: a square plate under in-plane compression and a cylindrical shell under pressure.

1. INTRODUCTION

In general, the postbuckling behaviour of plates and shells is computed by using standard predictor-corrector algorithms and branch switching techniques.¹⁻³ The most popularly used scheme is the Newton-Raphson method associated with a load control, a displacement control, or an arc length control.⁴⁻⁶ Although such methods are continuously being improved, for instance, with better predictors,^{7,8} they require long computation times as compared to a linear problem, and it is difficult to automatize the step-by-step procedure. Moreover, the imperfection sensitivity analysis requires very long computation times since one has to perform one step-by-step computation for each given imperfection.

An alternative method has been proposed by Damil and Potier-Ferry⁹ to compute the postbuckling of perfect or imperfect elastic structures in a cheap and automatic way. As in classical postbuckling theory,¹⁰⁻¹² the solution is sought by means of asymptotic expansions but without a too earlier truncature of the series. They established a proper way to expand, and showed how to compute all the terms of the series by building up and solving linear problems in a recurrent manner. Practically, the linear problems are solved by a classical finite element method and only few terms have to be computed. Since all the linear problems have the same stiffness matrix, only one matrix inversion is needed. This is a very attractive point of the method, which requires about the same computing time as a single step of the modified Newton-Raphson algorithm. This method had been illustrated on a one-dimensional test: the postbuckling of an

* Université Hassan II, Faculté des Sciences II, Casablanca, Maroc

imperfect elastic beam which rests on a non-linear foundation. It notably improves the classical perturbed bifurcation theory where only the first term of the expansion is considered.

This asymptotic-numerical method falls into the category of perturbation techniques that have already been addressed in References 13–19. In general, only a few terms of the series can be really determined because of the complexity of the expansion procedure, and, quite often, the perturbation technique is reduced to a second-order approximation. The use of symbolic computation software can be very helpful to circumvent this difficulty.¹⁸ In Reference 9 the governing equations of plate and shell models have been written in a simple form with quadratic nonlinearities. Hence, the expansion procedure is not too complex and explicit formulas have been derived for each individual term. The procedure can easily be implemented in an existing finite element software and it permits one to compute numerically as many terms as wanted.

The asymptotic-numerical method gives a continuous analytic representation of the solution branch which contrasts with the step-by-step representation given by predictor–corrector algorithms. Inside the radius of convergence of the series, the analytic representation can be very precise, provided that a sufficient number of terms are used and there is definitely no need of any correction. One drawback seems to be that the analytic representation is limited by a finite radius of convergence, but it would be a real drawback only if the radius of convergence was small, for instance, if it was smaller than the ‘step length’, as one can expect when using a classical step-by-step procedure. Furthermore, after an expansion process, various techniques can be applied, either for a direct improvement of polynomial representation of the solution branch²¹ or for constructing powerful numerical methods, by using the terms of the series as trial vectors in a Rayleigh–Ritz method.¹⁷

The aim of the present paper is to test our asymptotic-numerical method for computing the first bifurcating branch of a perfect plate or a perfect cylindrical shell. It is organized as follows.

In Section 2, we show that, within the framework of small strains and moderate rotations, the governing equations of a large class of plate and shell models are quadratic, and can be written in the form

$$L(\mathbf{U}) + (\lambda - \lambda_c)L'(\mathbf{U}) + Q(\mathbf{U}, \mathbf{U}) = 0 \quad (1)$$

where \mathbf{U} is a mixed stress–displacement unknown vector, λ the load parameter, λ_c the buckling load, L and L' are linear operators and Q a bilinear operator. This equation is similar to equation (6) of Reference 9, except for the term that accounts for the imperfection. In view of applying expansion techniques for computing a bifurcating branch at $\lambda = \lambda_c$, it is convenient to write the equilibrium equation in a simple quadratic form such as (1).

In Section 3, we present a review of the asymptotic-numerical method. First, we define proper expansions of the unknowns and introduce them into (1). So, the non-linear mixed problem (1) is transformed into a sequence of linear mixed problems that are written explicitly in Section 3.2. The next step consists in changing every linear mixed problem into a displacement problem, and to solve them by a standard finite element method.

The method is applied to a flat plate in Section 4 and to a cylindrical shell in Section 5. Computational techniques are discussed at that time, and it is shown how to implement the method in an existing finite element software. The combination of the asymptotic-numerical principle and the classical Fourier decomposition for axisymmetric geometry is detailed in Section 5.

In Section 6, we present the numerical results and discuss the radius of convergence of the series. We also give some insight into the various attempts made for the improvement of the method.

2. GOVERNING EQUATIONS

Various variational principles can be established to write the governing equations of plate and shell models. Hereafter, we recall that a pure displacement approach yields cubic governing equations, whereas the mixed stress–displacement approach yields only quadratic ones. Hence, in view of applying an expansion procedure, the mixed approach is preferred here since it leads to a simpler algebra. A pure displacement version of the present method would be practicable, but it is much more tedious. After the expansion process, we shall come back to a displacement formulation and use very classical displacement FEM. The aim of this section is to write the governing equations of a large class of plate and shell models under form (1).

The displacement of the middle surface of the shell or the plate will be denoted by U_α and W , where U_α are the in-plane displacements (plane (x_1, x_2)) and W is the transversal displacement in the x_3 direction (Figure 1). The Green–Lagrange strains are supposed to vary linearly through the thickness x_3 and will be denoted by

$$\Gamma(U_\alpha, W) + x_3 \mathbf{K}(U_\alpha, W) \quad (2a)$$

with

$$\Gamma(U_\alpha, W) = \Gamma^L(U_\alpha, W) + \Gamma^{NL}(U_\alpha, W) \quad (2b)$$

Γ and \mathbf{K} are the generalized membrane strain and bending strain. The membrane strain will be separated into a linear part $\Gamma^L(U_\alpha, W)$ and a non-linear part $\Gamma^{NL}(U_\alpha, W)$, whereas the bending strain \mathbf{K} is supposed to be linear with respect to the displacement (framework of moderate rotations).

For example, in the case of a Von Karman plate, the components of these generalized strain tensors are:

$$\Gamma_{\alpha\beta}^L = \frac{1}{2}(U_{\alpha,\beta} + U_{\beta,\alpha}) \quad (3a)$$

$$\Gamma_{\alpha\beta}^{NL} = \frac{1}{2}(W_{,\alpha} W_{,\beta}) \quad (3b)$$

$$K_{\alpha\beta} = -W_{,\alpha\beta} \quad (3c)$$

and in the case of a Donnell cylindrical shell of radius R we have the same components, except for the following one:

$$\Gamma_{22}^L = U_{2,2} - \frac{W}{R} \quad (4)$$

The membrane forces and the bending moments associated with Γ, \mathbf{K} will be denoted by \mathbf{N} and \mathbf{M} . We assume that the material is linear-elastic, and that there is no coupling between membrane

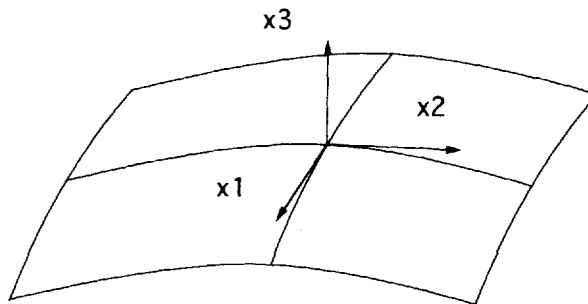


Figure 1. Reference configuration of the shell (or the plate)

and flexion in the constitutive equations:

$$\mathbf{N} = \mathbf{C}_m : \boldsymbol{\Gamma} \quad (5a)$$

$$\mathbf{M} = \mathbf{C}_b : \mathbf{K} \quad (5b)$$

The more general situation with a coupling matrix \mathbf{C}_{mb} between membrane and flexion is of great concern for unsymmetric composite laminates for example, but it has been reported in the Appendix for simplicity of this presentation.

The potential energy of the shell or the plate can be written as

$$P(U_\alpha, W) = \int_{\Omega} \mathcal{W}(\boldsymbol{\Gamma}, \mathbf{K}) \, d\Omega - \lambda \mathcal{P}(U_\alpha, W) \quad (6a)$$

with

$$\mathcal{W}(\boldsymbol{\Gamma}, \mathbf{K}) = \frac{1}{2} \boldsymbol{\Gamma} : \mathbf{C}_m : \boldsymbol{\Gamma} + \frac{1}{2} \mathbf{K} : \mathbf{C}_b : \mathbf{K} \quad (6b)$$

where \mathcal{W} is the strain energy density, λ the load parameter, and $\lambda \mathcal{P}$ the work done by the applied loads. Since $\boldsymbol{\Gamma}$ and \mathbf{K} are quadratic in U_α and W , $P(U_\alpha, W)$ is of degree 4 with respect to U_α, W . The equilibrium equations, derived from the constancy of $P(U_\alpha, W)$, are cubic in U_α, W , and cannot be put under the quadratic form (1). It is necessary to introduce additional variables to reduce the degree in the equations. This can be achieved by using the Hellinger–Reissner functional:

$$\text{HR}(U_\alpha, W, \mathbf{N}, \mathbf{M}) = \int_{\Omega} \boldsymbol{\Gamma} : \mathbf{N} + \mathbf{K} : \mathbf{M} - \mathcal{W}^*(\mathbf{N}, \mathbf{M}) \, d\Omega - \lambda \mathcal{P}(U_\alpha, W) \quad (7a)$$

with

$$\mathcal{W}^*(\mathbf{N}, \mathbf{M}) = \frac{1}{2} \mathbf{N} : \mathbf{C}_m^{-1} : \mathbf{N} + \frac{1}{2} \mathbf{M} : \mathbf{C}_b^{-1} : \mathbf{M} \quad (7b)$$

The mixed functional HR is cubic in $U_\alpha, W, \mathbf{N}, \mathbf{M}$ and the constancy of HR yields quadratic equations. It is important to note that the bending strain is linear with respect to the displacement and there is no need to introduce the variable \mathbf{M} here to get quadratic equations. We choose to eliminate this variable and keep U_α, W, \mathbf{N} only. So, the governing equations can be derived from the first variation of the functional

$$\mathcal{L}(U_\alpha, W, \mathbf{N}) = \int_{\Omega} \boldsymbol{\Gamma} : \mathbf{N} - \frac{1}{2} \mathbf{N} : \mathbf{C}_m^{-1} : \mathbf{N} + \frac{1}{2} \mathbf{K} : \mathbf{C}_b : \mathbf{K} \, d\Omega - \lambda \mathcal{P}(U_\alpha, W) \quad (8)$$

which yields quadratic equations in U_α, W, \mathbf{N} . By introducing the mixed unknown

$$\mathbf{U} = \begin{Bmatrix} U_\alpha \\ W \\ N_{\alpha\beta} \end{Bmatrix}$$

the governing equations of the model can be obtained from

$$\delta(\mathcal{L}(\mathbf{U})) = 0 \quad \forall \delta \mathbf{U} \quad (9)$$

We assume that the fundamental solution of (9) is linear with respect to the load parameter λ (linear prebuckling) (Figure 2). This is rigorously exact for a plate under in-plane compression and a common approximation for a cylindrical shell under pressure.²² We introduce the following change of variable which is classical within the postbuckling theory (see Reference 12, for instance):

$$\mathbf{U} = \lambda \mathbf{U}^0 + \hat{\mathbf{U}} \quad (10)$$

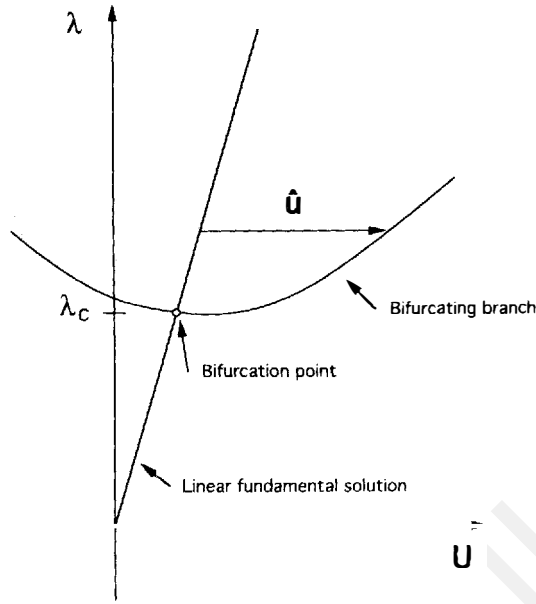


Figure 2. Load–displacement curve with a linear fundamental solution

where λ is the load parameter, \mathbf{U}° is the fundamental solution, and $\hat{\mathbf{U}}$ is the new unknown. Because there will be no possible confusion, we shall forget the sign $\hat{}$ in order to simplify the notation. From now onwards, \mathbf{U} will represent the difference between the actual displacement and the fundamental one.

With the change of variable (10), the governing equation (9) can be rewritten as

$$\langle\langle L(\mathbf{U}), \delta\mathbf{U} \rangle\rangle + (\lambda - \lambda_c) \langle\langle L'(\mathbf{U}), \delta\mathbf{U} \rangle\rangle + \langle\langle Q(\mathbf{U}, \mathbf{U}), \delta\mathbf{U} \rangle\rangle = 0 \quad \forall \delta\mathbf{U} \quad (11a)$$

with

$$\langle\langle L(\mathbf{U}), \delta\mathbf{U} \rangle\rangle = \int_{\Omega} \mathbf{N} : \delta\mathbf{\Gamma}^L + (\mathbf{\Gamma}^L - \mathbf{C}_m^{-1} : \mathbf{N}) : \delta\mathbf{N} + \mathbf{K} : \mathbf{C}_b : \delta\mathbf{K} \, d\Omega + \lambda_c \int_{\Omega} \mathbf{N}^\circ : \delta\mathbf{\Gamma}^{NL} \, d\Omega \quad (11b)$$

$$\langle\langle L'(\mathbf{U}), \delta\mathbf{U} \rangle\rangle = \int_{\Omega} \mathbf{N}^\circ : \delta\mathbf{\Gamma}^{NL} \, d\Omega \quad (11c)$$

$$\langle\langle Q(\mathbf{U}, \mathbf{U}), \delta\mathbf{U} \rangle\rangle = \int_{\Omega} \mathbf{\Gamma}^{NL} : \delta\mathbf{N} + \mathbf{N} : \delta\mathbf{\Gamma}^{NL} \, d\Omega \quad (11d)$$

$\langle\langle L(\cdot), \delta\mathbf{U} \rangle\rangle$ and $\langle\langle L'(\cdot), \delta\mathbf{U} \rangle\rangle$ are linear operators and $\langle\langle Q(\cdot, \cdot), \delta\mathbf{U} \rangle\rangle$ is a bilinear operator.

In view of a further finite element discretization, it is convenient to consider a variational formulation as (11a) rather than local equilibrium equations. Here the problem involves two bilinear forms $\langle\langle L(\mathbf{U}), \delta\mathbf{U} \rangle\rangle$, $\langle\langle L'(\mathbf{U}), \delta\mathbf{U} \rangle\rangle$ and one trilinear form $\langle\langle Q(\mathbf{U}, \mathbf{U}), \delta\mathbf{U} \rangle\rangle$. To be consistent with our classical operational notations (1), we have formally introduced a scalar product $\langle\langle \cdot, \cdot \rangle\rangle$ which classically allows one to associate linear self-adjoint operators L and L' with the two bilinear forms, and the quadratic operator Q with the trilinear form. But, at this stage, the scalar product is unnecessary.

3. REVIEW OF THE ASYMPTOTIC-NUMERICAL METHOD

For $\lambda = \lambda_c$, there is a solution branch that bifurcates from the fundamental one. This means that the tangent operator L is singular for this value of the parameter λ . Furthermore, we assume that the kernel of this tangent operator L is one-dimensional, what occurs generically. For structures of revolution, the eigenspace is two-dimensional, but it is known that, even in this case, all the bifurcating solutions can be obtained by one-mode analysis. The asymptotic-numerical method aims to get a large part of the bifurcating branch in the form of a polynomial approximation.

3.1. Polynomial approximation of a bifurcating branch

By use of the implicit function theorem, it is established that the unknown \mathbf{U} and the load parameter λ can be expanded into an integro-power series of a parameter 'a':

$$\lambda - \lambda_c = \sum_{p=1}^{\infty} C(p)a^p \quad (12a)$$

$$\mathbf{U} = \sum_{p=1}^{\infty} a^p \mathbf{V}(p) \quad (12b)$$

with $\mathbf{V}(p)$ orthogonal to $\mathbf{V}(1)$ for $p \geq 2$,

$$\langle\langle \mathbf{V}(p), \mathbf{V}(1) \rangle\rangle = 0 \quad \text{if } p \geq 2. \quad (12c)$$

This representation (12) of a bifurcating solution branch is classical within bifurcation theory. Here the unknown \mathbf{U} is not expressed as a function of the parameter λ , but it is the pair unknown-parameter (\mathbf{U}, λ) that is expressed as a function of the amplitude a , which is the projection of \mathbf{U} on the eigenmode $\mathbf{V}(1)$. It is clear that the so-defined amplitude a and the representation (12) depend on the chosen projector or, equivalently, on the chosen scalar product (12c).

The principle of the numerical method is to compute successively a number of vectors $\mathbf{V}(p)$ and coefficients $C(p)$ up to a given order n . The truncature of the series (12) at the same order n yields polynomials $\lambda(a, n)$, $\mathbf{U}(a, n)$, that we consider as approximations of the exact-solution branch.

3.2. Expansion of the non-linear problem into linear problems

By introducing expansions (12) into (11), we get a set of linear problems in $\mathbf{V}(p)$ and $C(p)$:

$$\langle\langle L(\mathbf{V}(1)), \delta\mathbf{U} \rangle\rangle = 0 \quad (13a)$$

$$\langle\langle L(\mathbf{V}(2)), \delta\mathbf{U} \rangle\rangle = -C(1)\langle\langle L'(\mathbf{V}(1)), \delta\mathbf{U} \rangle\rangle - \langle\langle Q(\mathbf{V}(1), \mathbf{V}(1)), \delta\mathbf{U} \rangle\rangle \quad (13b)$$

$$\langle\langle \mathbf{V}(2), \mathbf{V}(1) \rangle\rangle = 0$$

$$\begin{aligned} \langle\langle L(\mathbf{V}(3)), \delta\mathbf{U} \rangle\rangle = & -C(1)\langle\langle L'(\mathbf{V}(2)), \delta\mathbf{U} \rangle\rangle - C(2)\langle\langle L'(\mathbf{V}(1)), \delta\mathbf{U} \rangle\rangle \\ & - 2\langle\langle Q(\mathbf{V}(1), \mathbf{V}(2)), \delta\mathbf{U} \rangle\rangle \end{aligned} \quad (13c)$$

$$\langle\langle \mathbf{V}(3), \mathbf{V}(1) \rangle\rangle = 0$$

$$\langle\langle L(\mathbf{V}(p)), \delta\mathbf{U} \rangle\rangle = - \sum_{r=1}^{p-1} C(r)\langle\langle L'(\mathbf{V}(p-r)), \delta\mathbf{U} \rangle\rangle - \sum_{r=1}^{p-1} \langle\langle Q(\mathbf{V}(r), \mathbf{V}(p-r)), \delta\mathbf{U} \rangle\rangle \quad (13d)$$

$$\langle\langle \mathbf{V}(p), \mathbf{V}(1) \rangle\rangle = 0$$

Since the kernel of L is one-dimensional, the solution $\mathbf{V}(1)$ of (13a) depends on a single multiplier. Because of the representation (12b) and (12c) of the branch, this multiplier contributes to the definition of the parameter a , but it does not change the solution branch. Hence, it can be chosen arbitrarily, and, in what follows, we consider that the solution of (13a) is uniquely defined. Because L is singular, the RHS of the linear problems (13b)–(13d) must satisfy a solvability condition that is obtained by setting $\delta\mathbf{U} = \mathbf{V}(1)$ in these variational equations. In this way, we compute the coefficient $C(p)$ in terms of the vectors $\mathbf{V}(p')$, $p' < p$.

Equation (13b) leads to

$$C(1) = -\frac{\langle\langle Q(\mathbf{V}(1), \mathbf{V}(1)), \mathbf{V}(1) \rangle\rangle}{\langle\langle L'(\mathbf{V}(1)), \mathbf{V}(1) \rangle\rangle} \quad (14a)$$

and it follows from (13d) that

$$C(p-1) = \frac{1}{\langle\langle L'(\mathbf{V}(1)), \mathbf{V}(1) \rangle\rangle} \times \left[-\sum_{r=1}^{p-2} C(r) \langle\langle L'(\mathbf{V}(p-r)), \mathbf{V}(1) \rangle\rangle - \sum_{r=1}^{p-1} \langle\langle Q(\mathbf{V}(r), \mathbf{V}(p-r), \mathbf{V}(1)) \rangle\rangle \right] \quad (14b)$$

Formally, the solution of (13) is equivalent to the solution of a set of linear problems in $\mathbf{V}(p)$. The p th problem can be written under the more compact form

$$\langle\langle L(\mathbf{V}(p)), \delta\mathbf{U} \rangle\rangle = \langle\langle \mathbf{F}(p), \delta\mathbf{U} \rangle\rangle \quad \forall \delta\mathbf{U} \quad (15a)$$

$$\langle\langle \mathbf{V}(p), \mathbf{V}(1) \rangle\rangle = 0 \quad (15b)$$

The unknown vector $\mathbf{V}(p)$ includes the displacement and the membrane stress resultant as previously:

$$\mathbf{V}(p) = \begin{Bmatrix} U_\alpha(p) \\ W(p) \\ N_{\alpha\beta}(p) \end{Bmatrix} \quad (16)$$

The operator $\langle\langle L(\cdot), \delta\mathbf{U} \rangle\rangle$ is defined by (11b) and the RHS of (15a) can be made explicit from (13d), (11c) and (11d). For example, with Von-Karman-type non-linearity (see (3b)), we get

$$\langle\langle \mathbf{F}(p), \delta\mathbf{U} \rangle\rangle = \int_{\Omega} F_\alpha^U(p) \delta W_{,\alpha} + F_{\alpha\beta}^N(p) \delta N_{\alpha\beta} \, d\Omega \quad (17a)$$

where

$$F_\alpha^U(p) = -\sum_{r=1}^{p-1} (C(r) N_{\alpha\beta}^0 + N_{\alpha\beta}(r)) W_{,\beta}(p-r) \quad (17b)$$

$$F_{\alpha\beta}^N(p) = -\sum_{r=1}^{p-1} \frac{1}{2} W_{,\alpha}(r) W_{,\beta}(p-r) \quad (17c)$$

3.3. Transformation of the linear mixed problems into displacement problems

Let us recall that the variable \mathbf{V} contains not only the displacements U_α , W but also the stress $N_{\alpha\beta}$ which had been introduced to get quadratic non-linearities in the governing equations. As a consequence, all the linear problems (15a) are mixed. In order to use classical FEM, we shall

now transform (15) into a pure displacement problem and a pseudo-constitutive equation, which gives the p th term of the resultant stress $N(p)$ as a function of the displacement.

By choosing $\delta\mathbf{U}$ as a pure stress ($\delta U_\alpha = \delta W = 0$; $\delta N_{\alpha\beta} \neq 0$) in the linear problem (15a), we get the following pseudo-constitutive equation:

$$\mathbf{N}(p) = \mathbf{C}_m(\Gamma^L(p) - \mathbf{F}^N(p)) \quad (18)$$

Let us denote the displacement vector by

$$\bar{\mathbf{V}} = \begin{Bmatrix} U_\alpha \\ W \end{Bmatrix}$$

After having inserted (18) into (15a), we obtain a pure displacement problem

$$\langle\langle \bar{L}(\bar{\mathbf{V}}(p)), \delta\bar{\mathbf{U}} \rangle\rangle = \langle\langle \bar{\mathbf{F}}(p), \delta\bar{\mathbf{U}} \rangle\rangle \quad \forall \delta\bar{\mathbf{U}} \quad (19a)$$

$$\langle\langle \bar{\mathbf{V}}(p), \bar{\mathbf{V}}(1) \rangle\rangle = 0 \quad (19b)$$

with

$$\langle\langle \bar{L}(\bar{\mathbf{V}}(p)), \delta\bar{\mathbf{U}} \rangle\rangle = \int_{\Omega} (\Gamma^L : \mathbf{C}_m : \delta\Gamma^L + \mathbf{K} : \mathbf{C}_b : \delta\mathbf{K}) d\Omega + \lambda_c \int_{\Omega} \mathbf{N}^\circ : \delta\Gamma^{\text{NL}} d\Omega \quad (19c)$$

$$\langle\langle \bar{\mathbf{F}}(p), \delta\bar{\mathbf{U}} \rangle\rangle = \int_{\Omega} F_\alpha^U(p) \delta W_{,\alpha} + \mathbf{C}_m : \mathbf{F}^N(p) : \delta\Gamma^L d\Omega \quad (19d)$$

The operator $\langle\langle \bar{L}(\cdot), \delta\bar{\mathbf{U}} \rangle\rangle$ appears to be the sum of the elastic stiffness operator and the geometric stiffness operator.

So, the mixed problem (15) has been replaced by the displacement problem (19) and the formula (18) for the stress. Finally, \mathbf{N} is a convenient additional variable to reduce the degree in the equation and to make easier the expansion procedure. Once the non-linear problem is transformed into a set of linear problems, the stress \mathbf{N} is eliminated in these linear problems.

3.4. Solution of the linear problems using classical FEM

The last step of the asymptotic-numerical method is to solve successively the linear problems (19) in $\bar{\mathbf{V}}(p)$ and $C(p)$ with a very classical finite element method. After solving each problem, we compute the resultant stress $N(p)$ using formula (18). We find it easier to report the computational techniques in Sections 4 and 5, where we deal with a precise plate or a shell model, rather than in this general section.

A last remark should be made before closing this section. We have described the asymptotic procedure intentionally, on the basis of continuous formulations because this analysis requires one only to split between linear and quadratic operators. The finite element techniques are needed only for solving the linear problem (19).

4. APPLICATION TO VON KARMAN PLATE

4.1. Definition of the problem

We consider a geometrically perfect plate made of isotropic homogeneous material and loaded by in-plane forces (Figure 3). The middle surface of the plate is a symmetry plane for this problem and the fundamental solution is a pure membrane deformation without any lateral deflections. The first bifurcation is symmetric and the associated buckling mode is a pure bending deforma-

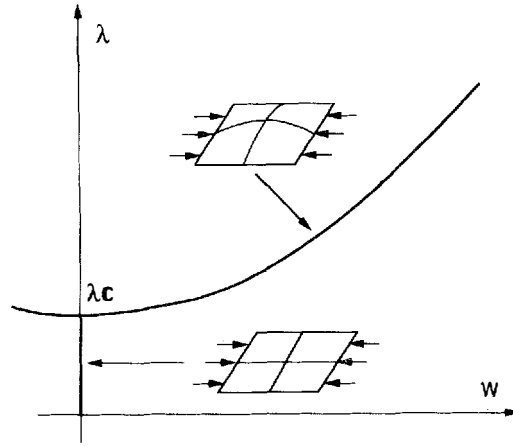


Figure 3. Pattern of the load-displacement curve for a plate under in-plane compression

tion. The vector $\mathbf{V}(1)$ solution of (13a) is the buckling mode:

$$\mathbf{V}(1) = \begin{Bmatrix} \bullet \\ W(1) \\ \bullet \end{Bmatrix} \quad (20)$$

Accounting for the symmetry of the problem, expansions (12) can be simplified into

$$\lambda - \lambda_c = C(2)a^2 + C(4)a^4 + C(6)a^6 + \dots \quad (21a)$$

$$\mathbf{U} = a \begin{Bmatrix} 0 \\ W(1) \\ 0 \end{Bmatrix} + a^2 \begin{Bmatrix} U_\alpha(2) \\ 0 \\ N_{\alpha\beta}(2) \end{Bmatrix} + a^3 \begin{Bmatrix} 0 \\ W(3) \\ 0 \end{Bmatrix} + a^4 \begin{Bmatrix} U_\alpha(4) \\ 0 \\ N_{\alpha\beta}(4) \end{Bmatrix} + a^5 \begin{Bmatrix} 0 \\ W(5) \\ 0 \end{Bmatrix} + \dots \quad (21b)$$

where a is a parameter which represents the projection of solution \mathbf{U} on the buckling mode. The coefficients $C(p)$ are zero when p is odd. $\mathbf{V}(p)$ is a pure membrane displacement when p is even and a pure flexion one if p is odd.

4.2. Computation of $\mathbf{V}(p)$ and $C(p)$ with FEM

As presented in Section 3, the mixed vector $\mathbf{V}(p)$ is computed in two steps. First, we calculate the displacement component $\bar{\mathbf{V}}(p)$ and, second, we calculate the stress component $N_{\alpha\beta}(p)$.

4.2.1. Computation of $\bar{\mathbf{V}}(p)$. With the classical notation of computational mechanics, the discretization of (19a) reads

$$[\mathbf{K}_e - \lambda_c \mathbf{K}_g][\bar{\mathbf{V}}(p)] = [\bar{\mathbf{F}}(p)] \quad (22)$$

where $[\bar{\mathbf{V}}(p)]$ is the vector of nodal displacements, $[\mathbf{K}_e]$ is the usual small-displacements stiffness matrix, $[\mathbf{K}_g]$ is the geometric stiffness matrix, $[\mathbf{K}_e - \lambda_c \mathbf{K}_g]$ is the tangent stiffness matrix at the bifurcation point and is singular. The orthogonality condition (19b) between $\bar{\mathbf{V}}(p)$ and $\bar{\mathbf{V}}(1)$ should be added to (22) in order to get an invertible problem. After discretization, this condition

reads

$$[\bar{V}(1)]^t [P] [\bar{V}(p)] = 0 \quad (23)$$

where P is a positive-definite matrix associated with the scalar product (19b). Here we choose to take $[P] = [K_e]$ to have an energy-oriented scalar product. So, (22) and (23) yield the invertible problem

$$\left[\begin{array}{c|c} K_e - \lambda_c K_g & \bar{V}^* \\ \hline \bar{V}^{*t} & 0 \end{array} \right] \left[\begin{array}{c} \bar{V}(p) \\ k \end{array} \right] = \left[\begin{array}{c} \bar{F}(p) \\ 0 \end{array} \right] \quad (24)$$

where $[\bar{V}^*] = [K_e][\bar{V}(1)]$ and k is a Lagrange multiplier. The construction of the global matrix in (24) requires very ordinary computation. The additional column \bar{V}^* has almost no consequence on the required storage dimension, and on the time decomposition if a compact column storage (skyline) is used. Note that the stiffness matrix is the same for all the linear problems. Hence, we perform a Crout decomposition once and for all.

The construction of the right-hand-side vector $[\bar{F}(p)]$ is very similar to the construction of a residual vector in a Newton–Raphson scheme, and it requires about the same computing time. Equations (3), (11), (13), (15), (17) and (19) yield

$$[\bar{F}(p)] = - \int_{\Omega} [B_0]^t [C_m] [F^N(p)] + [B_s]^t [F^U(p)] d\Omega \quad (25)$$

where $[B_0]$ and $[B_s]$ are the classical strain–displacement matrices defined by

$$[\Gamma^L] = [B_0][\bar{V}] \quad (26a)$$

$$[W_{,\alpha}] = [B_s][\bar{V}] \quad (26b)$$

4.2.2. Computation of $N_{\alpha\beta}(p)$. The membrane forces $N_{\alpha\beta}$ are calculated at each Gauss point by (18), which can be rewritten here as

$$N_{\alpha\beta}(p) = C_{m\alpha\beta\gamma\delta} \left(\Gamma_{\gamma\delta}^L(p) + \sum_{r=1}^{p-1} \frac{1}{2} W_{,\gamma}(r) W_{,\delta}(p-r) \right) \quad (27)$$

4.2.3. Computation of $C(p)$. By making explicit (14b), we get

$$C(p-1) = \frac{1}{\int_{\Omega} W_{,\alpha}(1) N_{\alpha\beta}^{\bullet} W_{,\beta}(1) d\Omega} \left[- \int_{\Omega} C_{m\alpha\beta\gamma\delta} \left[\sum_{r=1}^{p-1} \frac{1}{2} W_{,\gamma}(r) W_{,\delta}(p-r) \right] \Gamma_{\alpha\beta}^L(1) \right. \\ \left. + \left[\sum_{r=1}^{p-2} C(r) N_{\alpha\beta}^{\bullet} W_{,\alpha}(p-r) + \sum_{r=1}^{p-1} N_{\alpha\beta}(r) W_{,\alpha}(p-r) \right] W_{,\beta}(1) d\Omega \right] \quad (28)$$

4.3. Implementation

We have implemented this method in our homemade finite element program, which had been designed to perform linear buckling analysis, and non-linear continuation analysis with a Newton–Raphson scheme. Only few additional FORTRAN subroutines (that concern the construction of $[\bar{F}(p)]$) had to be introduced since $[K_e]$, $[K_g]$, λ_c , $\bar{V}(1)$ and the matrices $[B_0]$, $[B_s]$ were already available.

Once the buckling load λ_c and the corresponding buckling vector $\bar{V}(1)$ have been computed by a linear buckling analysis, this asymptotic-numerical method truncated at order n requires

- to assemble the matrix $\left[\begin{array}{c|c} \frac{K_e - \lambda_c K_g}{V^{*t}} & \bar{V}^* \\ \hline & 0 \end{array} \right]$
- to perform a Crout decomposition of the above matrix
- to assemble $n - 1$ RHS vectors $[\bar{F}(p)]$
- to perform $n - 1$ forward and backward substitutions

The computation of the coefficient $C(p - 1)$ and one term of the membrane stress $\mathbf{N}(p)$ can be judiciously performed during the assembling of $[\bar{F}(p)]$ so that almost no additional time is required for these quantities. In summary, we can say that this asymptotic-numerical method requires about the same computation time as a modified Newton-Raphson step with $n - 1$ iterations (without reactualization of the stiffness matrix).

In Table I, we compare the computation time of some vectors $V(p)$ with elastic analysis, buckling analysis and Newton-Raphson steps. For a large number of d.o.f., most of the computing time is spent in the Crout decomposition, and the asymptotic-numerical method is only one and a half times a linear elastic analysis.

4.4. Numerical results

We have tested this method on the academic problem of a simply supported square plate loaded by a uniform uniaxial compression. We use the triangular shell element D.K.T. due to Batoz *et al.*,²³ which has three nodes and five d.o.f. per node ($U_1, U_2, W, \theta_1, \theta_2$). For symmetry

Table I. Computing time of the asymptotic-numerical method. Comparison between linear elastic analysis, linear buckling analysis, and modified Newton-Raphson steps

	Number of d.o.f: 726		Number of d.o.f: 4812	
	Time in second (Workstation)	Ratio t/t elastic	Time in second (mini S-Comp)	Ratio t/t elastic
Crout decomposition of $K = Lt DL$	24	0.4	223	0.9
Linear elastic analysis	60	1	247	1
Modified Newton-Raphson step, 5 iterations	118	1.96	291	1.17
Linear buckling analysis	334	5.56	1870	7.57
Asymptotic-numerical method				
Order 2	85	1.41	270	1.09
Order 5	110	1.83	293	1.18
Order 10	169	2.81	333	1.34
Order 15	242	4.03	379	1.53

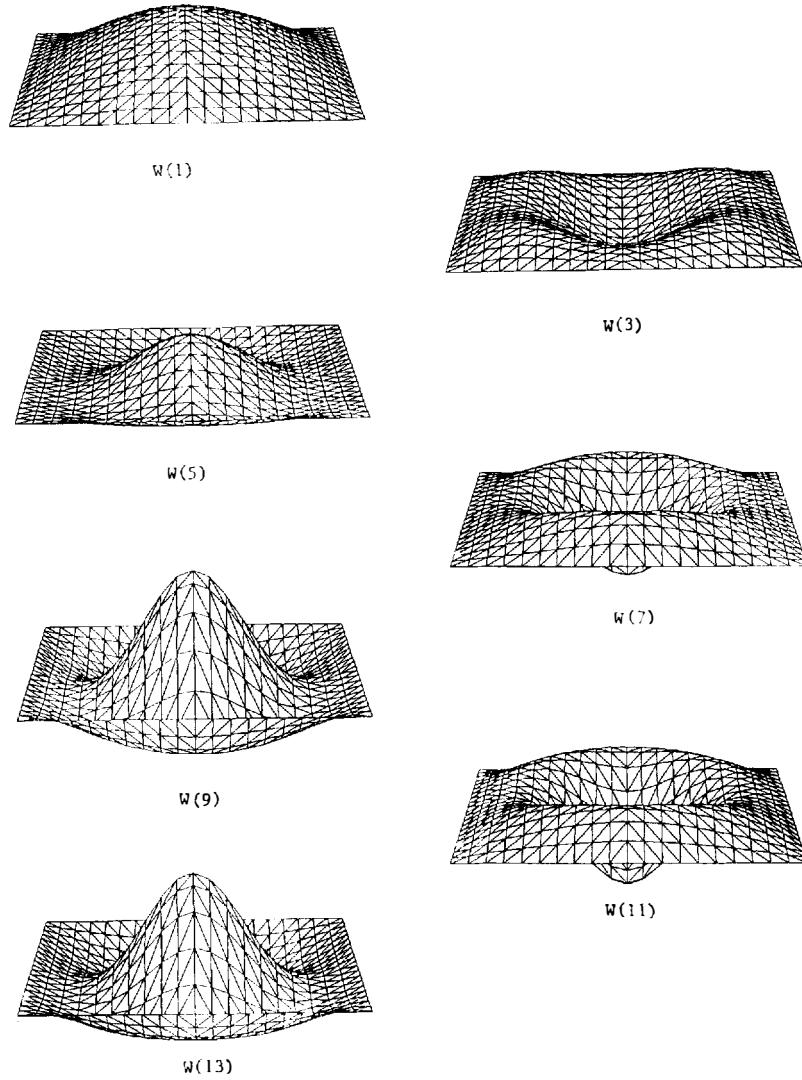
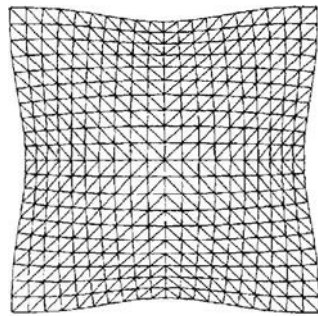


Figure 4. Visualization of the vectors $\vec{V}(p) = \{0, W(p)\}^T$ for p odd. Magnification factors have been used for those figures; see Table II for the real values of $W(p)/h$ at the centre of the plate

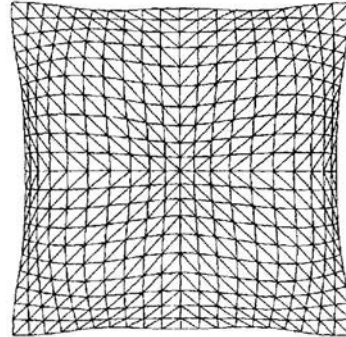
reasons, only a quarter of the plate was considered for computation (200 elements, 726 d.o.f.) but the whole plate is plotted in the figures.

The deflection $W(p)$ for the odd problems are shown in Figure 4 and the in-plane displacements $U_x(p)$ for the even problems in Figure 5. The coefficients $C(p)$ and the displacement $W(p)/h$ at the centre of the plate are reported in Table II.

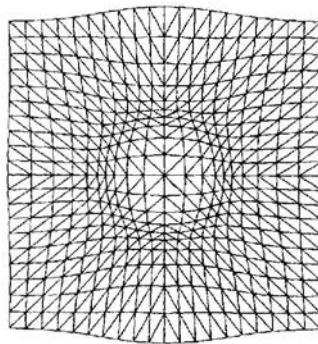
We have plotted that ratio W/h versus the ratio λ/λ_c for different truncatures of the series (21) in Figure 6. W is the deflection at the centre of the plate and h is the thickness of the plate. All these asymptotic curves are compared with the ‘exact’ solution obtained with a Newton–Raphson scheme. A discussion of the results is reported later in this paper, in order to be associated with the results on the cylindrical shell.



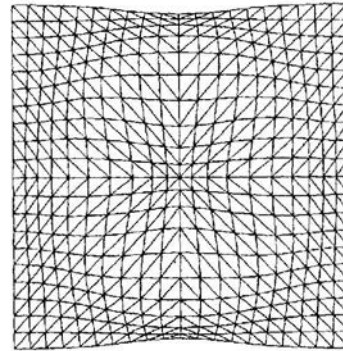
$u(2)$



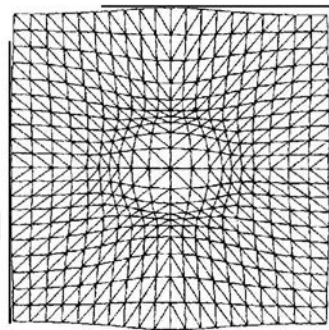
$u(4)$



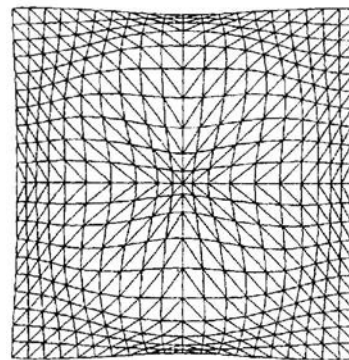
$u(6)$



$u(8)$



$u(10)$



$u(12)$

Figure 5. Visualization of the vectors $\bar{V}(p) = \{U_\alpha(p), \bullet\}$ for p even. Magnification factors have been used for these figures

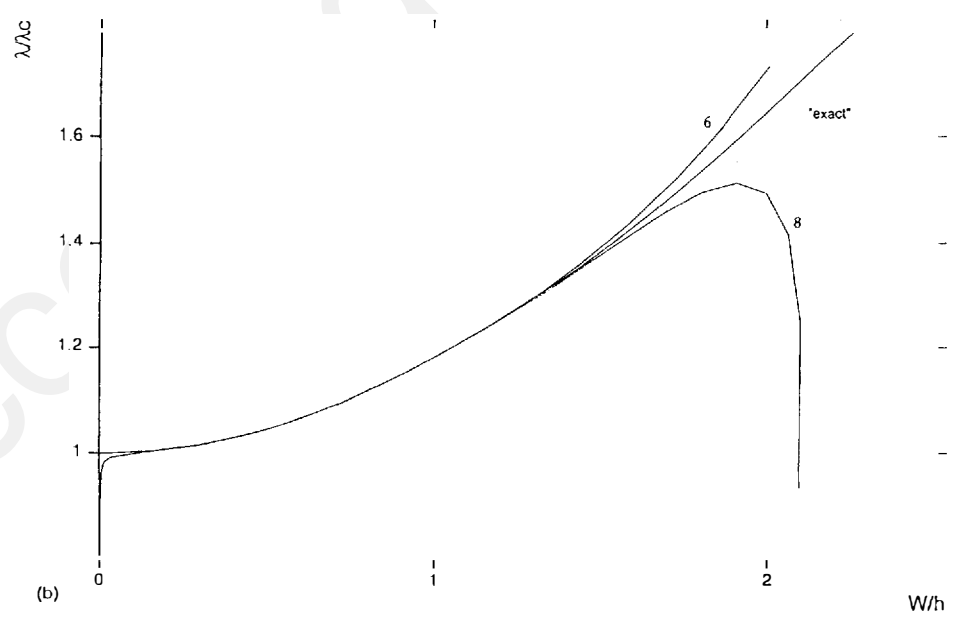
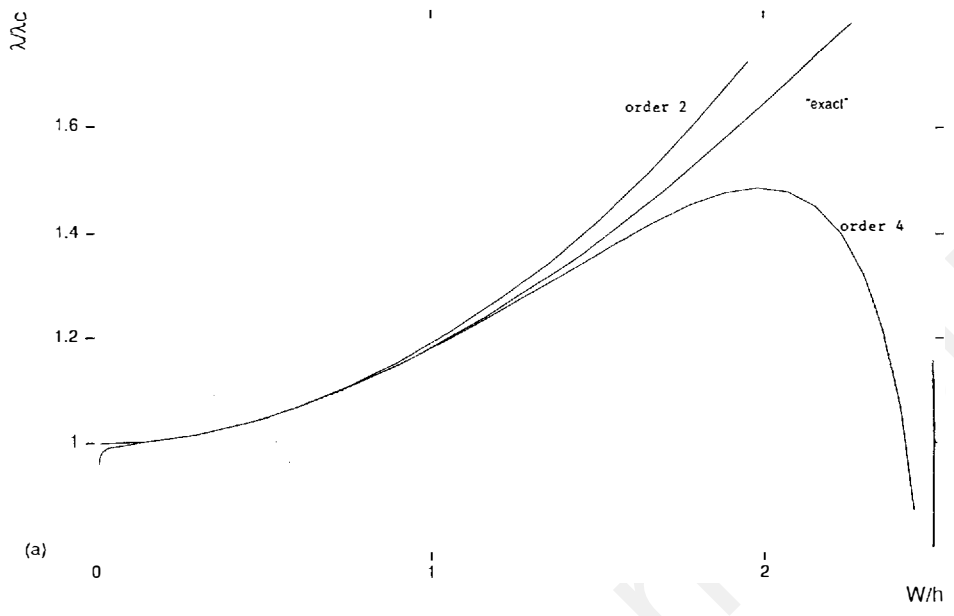


Figure 6.a, b

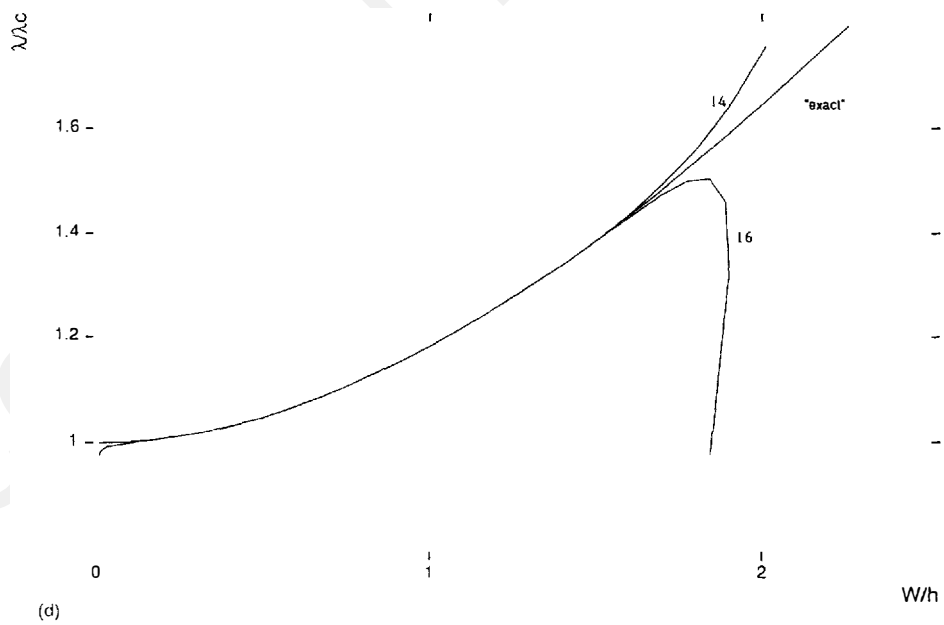
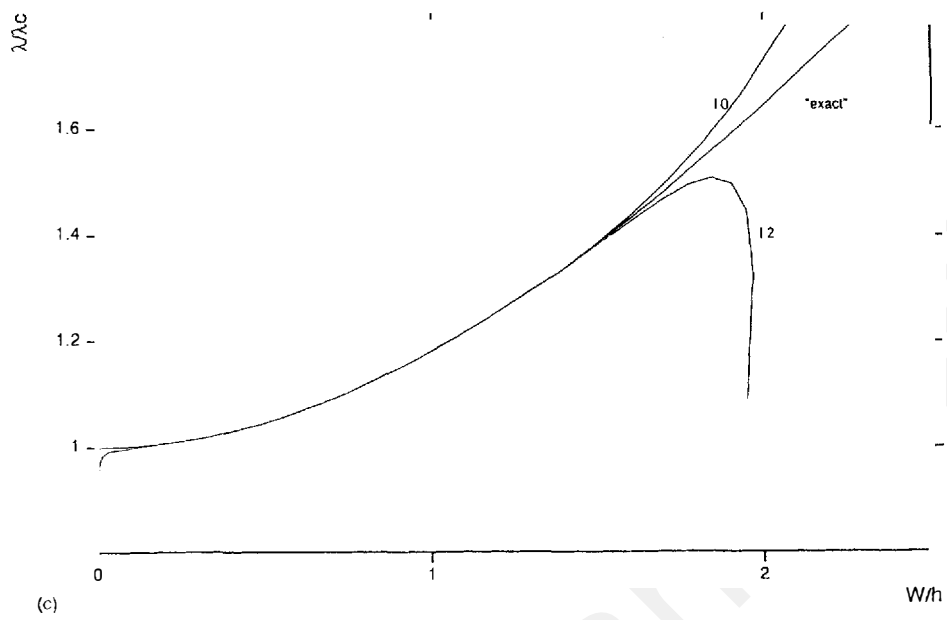


Figure 6. Load-displacement curve for the plate: W/h at the centre versus λ/λ_c . Comparison between the 'exact' solution and different truncatures of the asymptotic-numerical solution

Table II. Coefficients $C(p)$ and $W(p)/h$ at the centre for a square plate under uniaxial in-plane compression. The buckling mode is normalized by $W(1)/h=1$ at the centre of the plate

Coefficients of the load expansion		Coefficients of the displacement expansion at the centre of the plate	
$C(1)$	0	$W(1)/h$	1.00E+00
$C(2)$	0.189779	$W(2)/h$	0
$C(3)$	0	$W(3)/h$	-2.39E-02
$C(4)$	-0.0178759	$W(4)/h$	0
$C(5)$	0	$W(5)/h$	3.16E-03
$C(6)$	0.0027601	$W(6)/h$	0
$C(7)$	0	$W(7)/h$	-5.62E-04
$C(8)$	-0.0005163	$W(8)/h$	0
$C(9)$	0	$W(9)/h$	1.21E-04
$C(10)$	0.0001131	$W(10)/h$	0
$C(11)$	0	$W(11)/h$	-2.86E-05
$C(12)$	-0.0000267	$W(12)/h$	0
$C(13)$	0	$W(13)/h$	7.04E-06
$C(14)$	-0.0000066	$W(14)/h$	0

5. APPLICATION TO SHELLS OF REVOLUTION

5.1. Definition of the problem

Shell problems could also be studied within the previous method by using 2-D shell finite elements. However, for structures of revolution, the splitting into Fourier series permits us to limit ourselves to 1-D finite elements (see Reference 24, for instance), which is very efficient especially within the present asymptotic-numerical method.

For simplicity, we consider here only a circular cylindrical shell of radius R , length L and thickness h , which is made of a homogeneous isotropic elastic material. The co-ordinate system along the shell is shown in Figure 7: the axial displacement is denoted by U_1 , the circumferential one by U_2 and the radial one by W . The shell is subjected to an external pressure loading P .

Because of the symmetry of revolution, the buckling mode of the shell involves only one wave number. Unfortunately it is double, but we can restrict ourselves to a single-mode analysis without loss of generality.²⁵ Indeed, the eigenspace can be generated by rotation from one eigenmode, for instance, from the eigenmode that is symmetric with respect to the $(0, x_1, x_3)$ plane. According to this choice, the vector $\mathbf{V}(1)$ that is a solution of (13a) can be written as

$$\mathbf{V}(1) = 2 \begin{pmatrix} u_1(x) \cos(my/R) \\ u_2(x) \sin(my/R) \\ w(x) \cos(my/R) \\ n_{11}(x) \cos(my/R) \\ n_{22}(x) \cos(my/R) \\ n_{12}(x) \sin(my/R) \end{pmatrix} \quad (29)$$

where the integer m is the circumferential wave number of the buckling mode. The first bifurcation is symmetric and expansion (12) can be rewritten as

$$\lambda - \lambda_c = C(2)a^2 + C(4)a^4 + \dots \quad (30a)$$

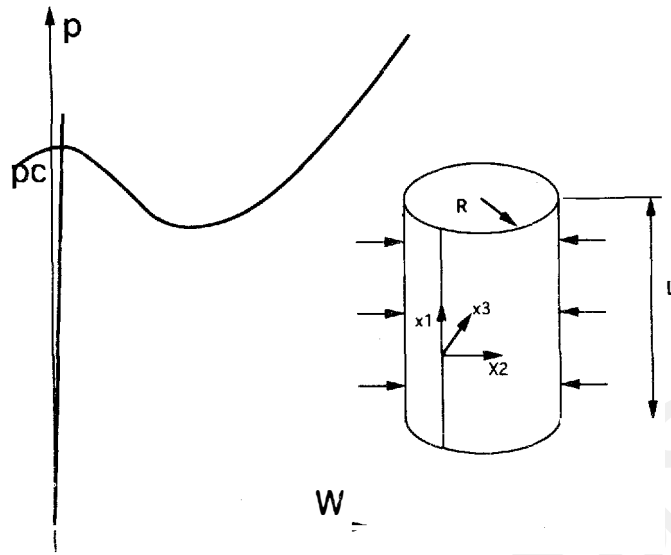


Figure 7. Pattern of the load-displacement curves for a cylindrical shell under pressure

$$\mathbf{U} = a \begin{Bmatrix} U_{\alpha}(1) \\ W(1) \\ N_{\alpha\beta}(1) \end{Bmatrix} + a^2 \begin{Bmatrix} U_{\alpha}(2) \\ W(2) \\ N_{\alpha\beta}(2) \end{Bmatrix} + \dots \quad (30b)$$

The coefficients $C(p)$ are zero if p is odd, but there is no particular property for the vectors $\mathbf{V}(p)$ as for the case of a plate, because the buckling mode involves both membrane and bending strains.

5.2. Computation of $\mathbf{V}(p)$ and $C(p)$ by FEM

For the computation of $\mathbf{V}(p)$ and $C(p)$, we could follow exactly the general procedure described in Sections 3 and 4, by solving problems (19) with 2-D shell elements. This would require to invert a single stiffness matrix whose dimension corresponds to a two-dimensional discretization of the shell. However, it is classical when there is a symmetry of revolution to introduce a circumferential Fourier series decomposition of the unknowns, and to split a 2-D problem into a set of 1-D problems for each harmonic. This requires one to discretize only the generatrix of the cylinder with 1-D elements. So, important computing time can be saved, provided that the amount of 1-D problems is not too large.

In our case, we have to solve not only one 2-D problem but a set of 2-D problems, and each 2-D problem has to be split into a set of 1-D problems. However, the number of 1-D problems to be solved is rather small as shown in the following. So, the combination of both asymptotic expansions and Fourier decomposition is very efficient with regard to computation time.

5.2.1. Splitting of the operators L, L', Q . In order to transform (13) into a set of 1-D problems, we need to split the 2-D operators $L(\cdot), L'(\cdot), Q(\cdot, \cdot)$ into 1-D operators for each harmonic. Let us use capital letters for 2-D operators and variables, and small letters for 1-D operators and variables. In order to avoid a heavy algebra with the function sines and cosines, we prefer to use

the complex exponential (we note that $i^2 = -1$). This leads us to consider complex-valued functions and to replace the scalar product by a Hermitian product in a classical way. In the same manner, we replace here the bilinear forms $\langle\langle L(\mathbf{U}), \delta\mathbf{U} \rangle\rangle$, $\langle\langle L'(\mathbf{U}), \delta\mathbf{U} \rangle\rangle$ and the trilinear form $\langle\langle Q(\mathbf{U}, \mathbf{U}), \delta\mathbf{U} \rangle\rangle$ by sesquilinear forms: to achieve this, it is sufficient to replace $\delta\mathbf{U}$ by its complex conjugate in the RHS of (11b)–(11d).

We shall say that the vector field $\mathbf{V}(x, y)$ is a pure harmonic of order k ($k > 0$) if it can be expressed in the following form:

$$\mathbf{V}(x, y) = \begin{pmatrix} u_1(x) \\ -iu_2(x) \\ w(x) \\ n_{11}(x) \\ n_{22}(x) \\ -in_{12}(x) \end{pmatrix} \exp(iky/R) \quad (31)$$

Such a pure harmonic is completely defined by k ($k > 0$) and a corresponding 1-D vector field $\mathbf{v}(x)^t = \{u_1(x), u_2(x), w(x), n_{11}(x), n_{22}(x), n_{12}(x)\}$ that is real-valued. The conjugate of a pure harmonic of order k will be called a pure harmonic of order $-k$. Let $\mathbf{V}(x, y)$, $\mathbf{V}'(x, y)$, $\mathbf{V}''(x, y)$ be pure harmonics of order k, k', k'' . If the operators L, L' and Q are considered as partial differential operators whose coefficients do not depend on y , they obviously satisfy the following splitting properties:

$$L(\mathbf{V}(x, y)) = l_k(\mathbf{v}(x)) \exp(iky/R) \quad (32a)$$

$$L'(\mathbf{V}(x, y)) = l'_k(\mathbf{v}(x)) \exp(iky/R) \quad (32b)$$

$$Q(\mathbf{V}(x, y), \mathbf{V}'(x, y)) = q_{k,k'}(\mathbf{v}(x), \mathbf{v}'(x)) \exp(i(k+k')y/R) \quad (32c)$$

which define real-valued linear (or bilinear) operators $l_k(\cdot), l'_k(\cdot), q_{k,k'}(\cdot, \cdot)$ acting on functions of the single variable x . The variational form of the latter splitting properties (32) can be written as:

$$\langle\langle L(\mathbf{V}), \mathbf{V}' \rangle\rangle = 0 \quad \text{if } k \neq k' \quad (33a)$$

$$\langle\langle L'(\mathbf{V}), \mathbf{V}' \rangle\rangle = 0 \quad \text{if } k \neq k' \quad (33b)$$

$$\langle\langle Q(\mathbf{V}, \mathbf{V}'), \mathbf{V}'' \rangle\rangle = 0 \quad \text{if } k + k' \neq k'' \quad (33c)$$

$$\langle\langle L(\mathbf{V}), \mathbf{V}' \rangle\rangle = \langle l_k(\mathbf{v}), \mathbf{v}' \rangle \quad \text{if } k = k' \quad (33d)$$

$$\langle\langle L'(\mathbf{V}), \mathbf{V}' \rangle\rangle = \langle l'_k(\mathbf{v}), \mathbf{v}' \rangle \quad \text{if } k = k' \quad (33e)$$

$$\langle\langle Q(\mathbf{V}, \mathbf{V}'), \mathbf{V}'' \rangle\rangle = \langle q_{k,k'}(\mathbf{v}, \mathbf{v}'), \mathbf{v}'' \rangle \quad \text{if } k + k' = k'' \quad (33f)$$

The splitting properties (33) are trivially established and will permit us to split each linear 2-D problem (13) into several 1-D problems.

5.2.2. Computation of $\mathbf{V}(p)$. According to the notation given by (31), we can rewrite the buckling mode (29) as

$$\mathbf{V}(1) = \mathbf{V}(1, 0) + \mathbf{V}(0, 1) \quad (34)$$

where $\mathbf{V}(1, 0)$ and $\mathbf{V}(0, 1)$ are pure harmonics of order m and $-m$, respectively, and they are both associated with the real 1-D vector field $\mathbf{v}(1, 0)(x)$. Note that $\mathbf{V}(0, 1)$ is the conjugate of $\mathbf{V}(1, 0)$.

Order 2: The RHS of (13b) is quadratic with respect to $\mathbf{V}(1)$. Hence, it can be split into pure harmonics of order $2m, 0, -2m$, and the solution $\mathbf{V}(2)$ is also of the form

$$\mathbf{V}(2) = \mathbf{V}(2, 0) + \mathbf{V}(1, 1) + \mathbf{V}(0, 2) \quad (35)$$

where these three vectors are pure harmonics of order $2m, 0, -2m$. Let the real 1-D vector field $\mathbf{v}(2, 0)$ correspond to $\mathbf{V}(2, 0)$ and $\mathbf{V}(0, 2)$, and let the real 1-D vector field $\mathbf{v}(1, 1)$ correspond to $\mathbf{V}(1, 1)$.

By choosing δU as a pure harmonics of order $2m$ and 0 , and with account taken of the splitting properties (33), we get the solution (35) of the 2-D problem (13b) by solving the two following 1-D problems:

$$\langle l_{2m}(\mathbf{v}(2, 0)), \delta \mathbf{u} \rangle = - \langle q_{m, m}(\mathbf{v}(1, 0), \mathbf{v}(1, 0)), \delta \mathbf{u} \rangle \quad \forall \delta \mathbf{u} \quad (36a)$$

$$\langle l_{\bullet}(\mathbf{v}(1, 1)), \delta \mathbf{u} \rangle = - 2 \langle q_{m, -m}(\mathbf{v}(1, 0), \mathbf{v}(1, 0)), \delta \mathbf{u} \rangle \quad \forall \delta \mathbf{u} \quad (36b)$$

The third problem to define $\mathbf{V}(0, 2)$ (by choosing δU as a pure harmonic of order $-2m$) is superfluous since this vector is a conjugate of $\mathbf{V}(2, 0)$. The 2-D orthogonality between $\mathbf{V}(1)$ and $\mathbf{V}(2)$ is automatically satisfied.

The two problems (36) are mixed and they are solved in two steps as presented in Section 3.2. After discretization of the generatrix of the cylinder with 1-D elements, the displacement parts of the vectors $\mathbf{v}(2, 0)$ and $\mathbf{v}(1, 1)$ are given by

$$[k_c(2m) + \lambda_c k_g(2m)] [\bar{v}(2, 0)] = [\bar{f}(2, 0)] \quad (37a)$$

$$[k_c(0) + \lambda_c k_g(0)] [\bar{v}(1, 1)] = [\bar{f}(1, 1)] \quad (37b)$$

Note that the tangent stiffness matrices in (37) are invertible. Indeed, it is only the matrix $[k_c(m) + \lambda_c k_g(m)]$ that corresponds to pure harmonics of order m that is singular. Because the operators l, q are real-valued, the matrices and RHS in (37) are real. After solving (37), we compute the membrane stress $n_{\alpha\beta}(2, 0)$ and $n_{\alpha\beta}(1, 1)$.

The splitting of (13c) (order 3) is left to the reader and we now detail the splitting of (13d) (order p).

Order p : We look for the vector $\mathbf{V}(p)$ as a sum of $p + 1$ vectors $\mathbf{V}(p - j, j)$ that are pure harmonics. The notations are such that the sum of the indices indicates the order p , and the difference of the indices indicates the order of the harmonic:

$$\mathbf{V}(p) = \sum_{j=\bullet}^p \mathbf{V}(p - j, j). \quad (38)$$

$\mathbf{V}(j, p - j)$ is the conjugate of $\mathbf{V}(p - j, j)$, and these two vectors are associated with the real 1-D vector $\mathbf{v}(p - j, j)$.

Each vector $\mathbf{v}(p - j, j)$ is a solution of the 1-D variational problem

$$\begin{aligned} \langle (l_{(p-2j)m}(\mathbf{v}(p-j, j)), \delta \mathbf{u}) \rangle = & - \sum_{r=1}^{\text{Int}(p-1)/2} C(2r) \langle (l'_{(p-2j)m}(\mathbf{v}(p-j-r, j-r)), \delta \mathbf{u}) \rangle \\ & - \sum_{r=1}^{p-1} \sum_{s=0}^r \langle (q_{(p-2j-r+2s)m, (r-2s)m}(\mathbf{v}(p-j-r+s, j-s), \mathbf{v}(r-s, s)), \delta \mathbf{u}) \rangle \quad \forall \delta \mathbf{u} \quad (39) \end{aligned}$$

with the convention that $\mathbf{v}(p, q) = \mathbf{v}(q, p)$, and $\mathbf{v}(p, q) = 0$ if $p < 0$ or $q < 0$. After discretization, the displacement part of $\mathbf{v}(p - j, j)$ is a solution of

$$[k_c((p-2j)m) + \lambda_c k_g((p-2j)m)] [\bar{v}(p-j, j)] = [\bar{f}(p-j, j)] \quad (40)$$

which is an invertible problem, except when $p - 2j = 1$. In such cases, the 2-D orthogonality between $\mathbf{V}(p)$ and $\mathbf{V}(1)$ yields a 1-D orthogonality condition between $\mathbf{v}(p - j, j)$ and $\mathbf{v}(1, 0)$. It is added to (40) as presented in Section 4.2 to get an invertible problem.

5.2.3. *Computation of $C(p)$.* The linear problem (39) is singular when $p - 2j = 1$, that is to say, for $p = 2k + 1$ and $j = k$ (k an integer). In this case, the RHS of (39) has to verify a solvability condition which determines the coefficient $C(2k)$. From equation (39) we get

$$C(2k) = \frac{1}{\langle l'_m(\mathbf{v}(1, 0)), \mathbf{v}(1, 0) \rangle} \left[- \sum_{r=1}^{k-1} C(2r) \langle l'_m(\mathbf{v}(k+1-r, k-r), \mathbf{v}(1, 0)) \rangle \right. \\ \left. - \sum_{r=1}^{2k} \sum_{s=0}^r \langle q_{(1-r+2s)m, (r-2s)m}(\mathbf{v}(k+1-r+s, k-s), \mathbf{v}(r-s, s)), \mathbf{v}(1, 0) \rangle \right] \quad (41)$$

5.3. Implementation

The combination of the asymptotic expansion technique and the splitting into harmonics leads to solve a set of 1-D linear problems. More precisely, the computation of expansion (30) up to order $p = 2k$ requires

- to assemble $2k + 1$ small matrices that correspond to the one-dimensional operators $l_0, l_m, l_{2m}, \dots, l_{(2k)_m}$, and
- to assemble $(k + 1)^2 - 2$ RHS vectors, and to solve $(k + 1)^2 - 2$ linear problems, with the $2k + 1$ above-mentioned stiffness matrices.

Note that the matrix $[(k_e(m) + \lambda_c k_g(m))]$ associated with the operator l_m is singular, and a column vector $[\mathbf{v}^*]$ is added as in (24) to get an invertible matrix.

The programming of the method is here more intricate than if we had simply used 2-D elements. But, as a result, the computing time is very short.

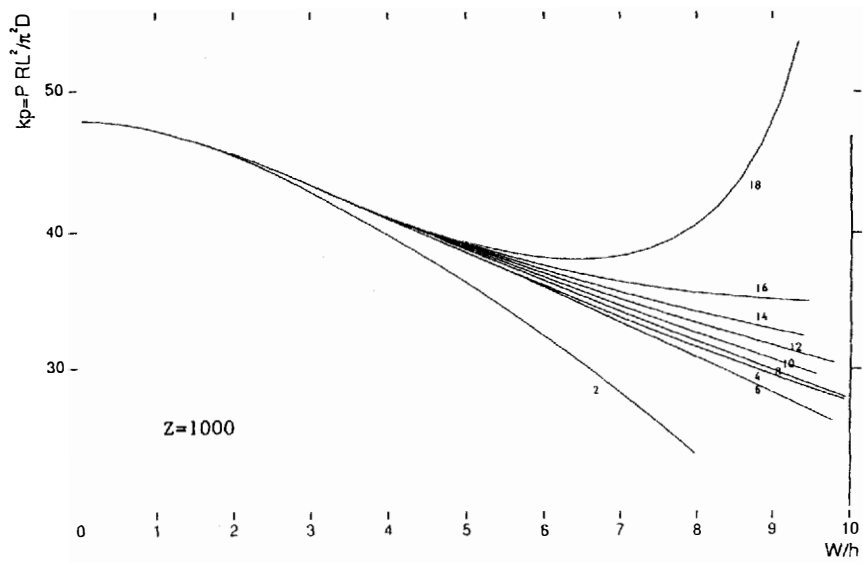
5.4. Numerical results

We have performed several tests for different geometries of a cylindrical shell loaded by external pressure. In fact, for buckling and postbuckling analysis, the geometry of a circular cylindrical shell can be characterized by the unique Bartdorf parameter $Z = \sqrt{1 - \nu^2} L^2 / Rh$ (Reference 20) which, for a given radius R and thickness h , represents the length of the shell. The generatrix of the cylinder has been discretized using classical 1-D elements with two nodes and the four degrees of freedom u_1, u_2, w, w_x . The results are presented in Figures 8–10, where the displacement w/h is reported versus the load parameter $k_p = P(RL^2/\pi^2 D)$ (P : pressure, $D = Eh^3/12(1 - \nu^2)$). Following Yamaki,²² we have tested different Z values. These results are discussed in Section 6.

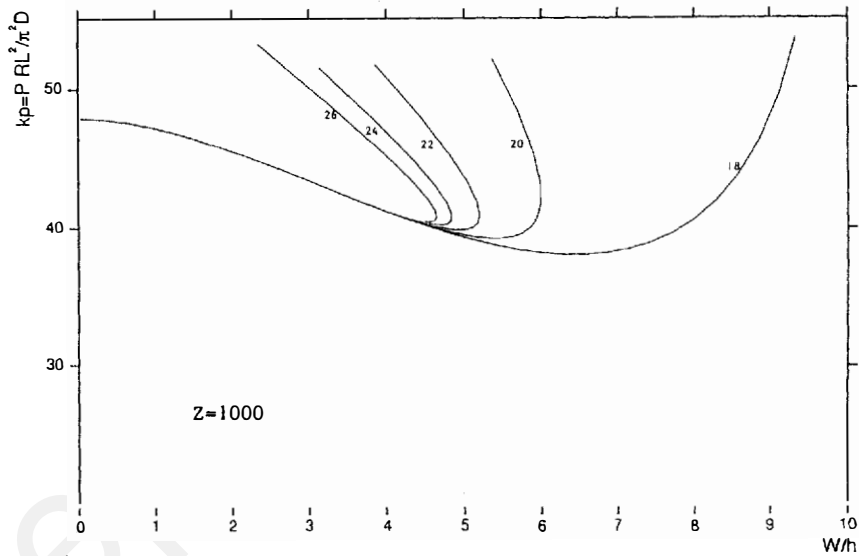
6. DISCUSSION OF THE NUMERICAL RESULTS

6.1. Pattern of the load–displacement curves

The load–displacement curves obtained for the plate and the cylindrical shell problems are very characteristic of polynomial approximations. Indeed, for small values of the parameter a , the asymptotic-numerical solutions (12) coincide quite perfectly with the exact solution, and if the order of truncature is sufficiently large they do not depend on this order of truncature. Beyond a critical value of ‘ a ’, the truncated polynomial series separates from the solution and they do not converge when the order of truncature increases. Obviously, this critical value is the radius of convergence of the series (12) and it is clearly defined in all the cases that we have studied



(a)



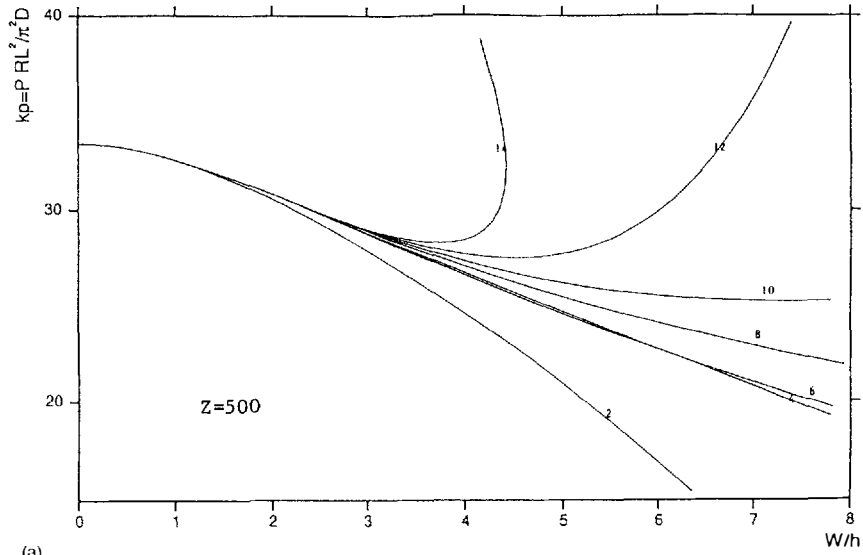
(b)

Figure 8. Load-displacement curve for the shell $Z = 1000$. w/h versus k_p . Different truncatures of the asymptotic-numerical solution

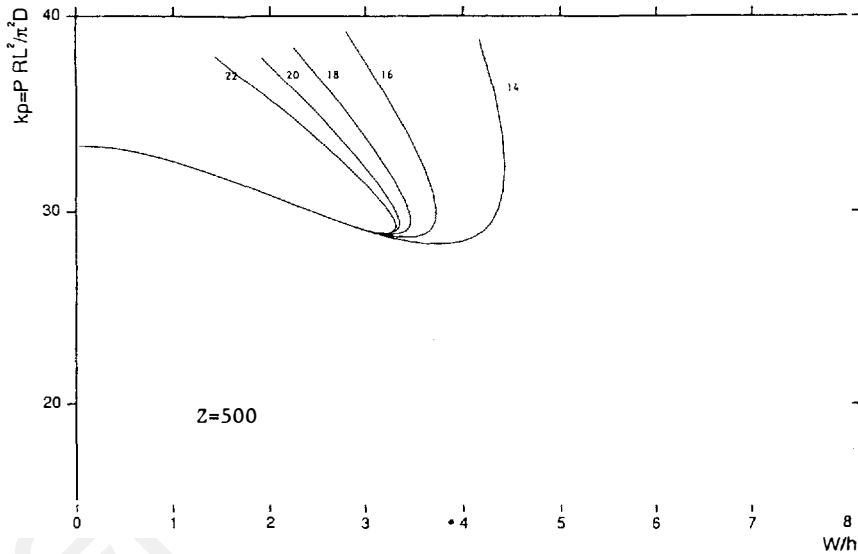
(see Figures 6–10). This typical pattern is due to the representation by polynomials because the functions a^n (n large) are almost zero if $a < 1$ and grow very rapidly for $a > 1$.

6.2. The radius of convergence

For the plate problem of Section 4, presented in Figures 4–6, we can see that the truncations of the series (21) at orders 4, 6, 8 and 10 significantly improve the solution at order 2, which is the



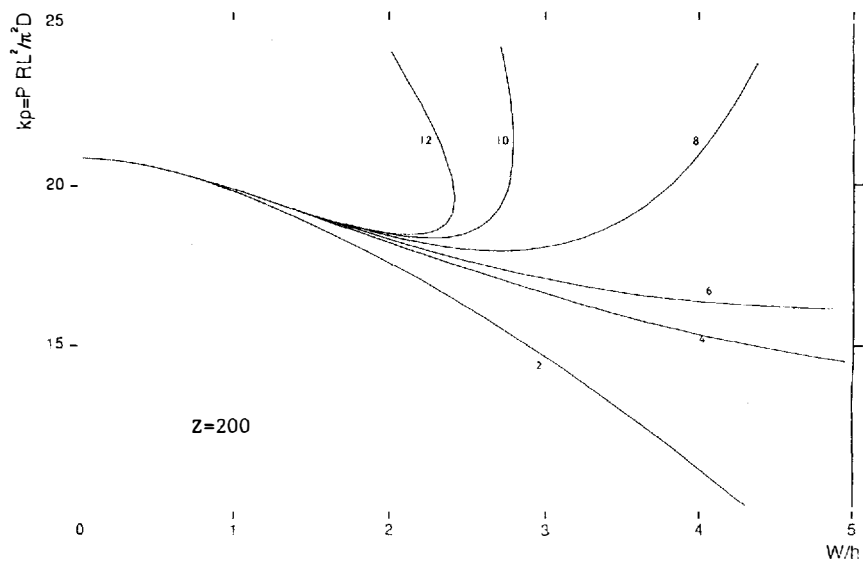
(a)



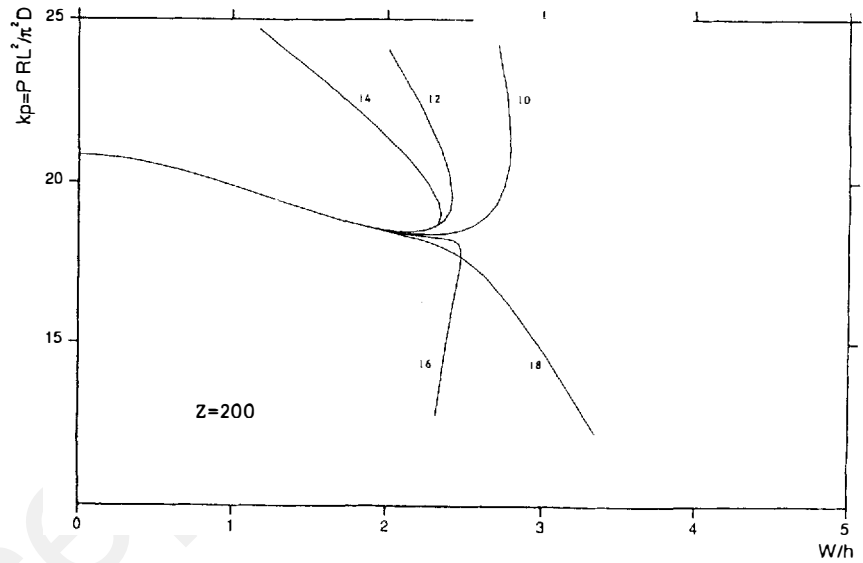
(b)

Figure 9. Load-displacement for the shell $Z = 500$. w/h versus k_p . Different truncatures of the asymptotic-numerical solution

classical initial postbuckling approximation. However, with the representation (21), it does not seem worth computing much more terms since little improvement is obtained after order 10. The radius of convergence is about $\lambda/\lambda_c = 1.4$ and $w/h = 1.6$ and it is 'reached' with about 10 terms in the expansions. After order 10, the vector $\mathbf{V}(p)$ for p odd and even, respectively, is almost rigorously collinear, as can be seen in Figures 4 and 5. We have tested other plate problems by changing the boundary conditions (clamped, simply supported, free), the shape of the plate (circular, rectangular) and the compressive load, and we found that the radius of convergence was



(a)



(b)

Figure 10. Load-displacement for the shell $Z = 200$. w/h versus k_p . Different truncatures of the asymptotic-numerical solution

not significantly modified. It varies between 1.4 and 1.6 for λ/λ_c and between 1.5 and 1.8 for w/h . We have also tested the influence of the mesh size by using 8, 50, 200 and 800 elements for a quarter of a square plate. We found that the radius of convergence does not depend on the mesh size and that the asymptotic-numerical expansions always converge to the 'exact' numerical solution associated with the same mesh. (The 'exact' solution mentioned here is in fact a finite element approximation of the plate problem and it varies with the mesh size.)

For the cylindrical shell, we do not report any exact solution, but we can clearly see the radius of convergence (Figures 8–10) when all the curves are separated from each other. For $Z = 1000$ (long shell), the radius of convergence is $P/P_c = 0.85$ and $w/h = 4$. For $Z = 500$, we get $P/P_c = 0.85$ and $w/h = 3$; and for $Z = 200$, we have $P/P_c = 0.8$ and $w/h = 2$. So, the radius of convergence in terms of P/P_c does not significantly depend on the geometrical parameter Z , whereas it clearly depends on Z in terms of w/h . This is consistent with the fact that the non-linear effects appear earlier for shorter shells.²² Smaller values of Z have not been tested here because the prebuckling solution is no more linear as it is supposed in this paper [equations (9) and (10)]. The account of such a non-linear prebuckling will be presented in a separate paper.

From a practical point of view, it is necessary to determine the radius of convergence. This can be done using classical techniques²¹ or by simply computing residual vectors for given values of the parameter a . Note that inside the radius of convergence, representation (12) yields a very precise approximation of the branch.

6.3. Increasing the range of validity

Already now, we are able to get a large part of the bifurcating branch for about the same computing time as one step of the modified Newton Raphson algorithm. Although this result is appreciable, one can be disappointed in that the radius of convergence is not larger. This is particularly true for the cylindrical shell where the minimum of the load–displacement curve, which is very important from an engineering point of view, is out of the radius of convergence. Hence, increasing the range of validity of the asymptotic-numerical method has become our major research axis. In this respect, we have investigated several variants of the present method on the plate problem. First, the choice of the scalar product (12c), which defines the orthogonality condition between the buckling mode $V(1)$ and all the other terms $V(p)$, may influence the radius of convergence. For the plate problem, we have tested different scalar products by setting the matrix P of (23) to identity, or to K_e , or to $K_e + \alpha K_g$ ($0 < \alpha < \lambda_c$). The variation of the radius of convergence was not determinant, and we recommend to take $P = K_e$ because of its mechanical sense, even if it is not always the best choice. We have also numerically applied the so-called Lyapunov–Schmidt reduction,¹² where the displacement is expanded with respect to both the buckling-mode amplitude a and the load λ . This leads to solve a set of linear problems and a single non-linear equation (bifurcation equation) in a and λ . Such a method requires more computations than the one presented here because the number of linear problems to be solved grows as N^2 (N order of truncature) and, furthermore, one non-linear equation is to be solved numerically. In comparison with representation (12), the Lyapunov–Schmidt reduction avoids solving the bifurcation equation by means of expansions, which could reduce the radius of convergence. Unfortunately, the improvements were not impressive enough to go further in that direction.

In fact, a very promising approach consists in rewriting *a posteriori* our asymptotic expansions, replacing polynomial truncatures by rational fractions called Padé approximants (see, for instance, Reference 26). Increasing of the range of validity can be very spectacular. For instance, a first test on the plate problem shows that we can get a very good approximation of the solution up to $\lambda/\lambda_c = 4$ and $w/h = 5$, with very little additional computation time. A survey of this very important point will be presented in a forthcoming paper.

Another direction of investigation would be to apply the reduced basis technique of Noor and Peters.¹⁷ The idea is to use the computed vector $V(p)$ as a Ritz basis, and to apply a classical Ritz (or Galerkin) method. In other words, the expansion procedure is used only for building up a suitable basis.

7. CONCLUSIONS

In this paper, we have applied an asymptotic-numerical method for computing the post-buckling behaviour of elastic plates and shells. The principle of the method is to compute numerically two polynomial series that give the displacement and the load as a function of the buckling-mode amplitude. By using a mixed approach, the governing equations have been written with a quadratic non-linearity. Hence, the expansion procedure is rather simple and it can easily be implemented in an existing FE software. It permits one to compute a very large number of terms of the series.

In comparison with a more classical step-by-step procedure, the present method has the following advantages:

- It is very efficient with regard to computation time. Indeed, the expansion technique transforms the non-linear problem into a sequence of linear problems with a single stiffness matrix. Hence, the computation time is of the same order as for a single step of the modified Newton–Raphson algorithm.
- The solution branch is known continuously and not only on some points.
- Another very important point is that the computation of the series is fully automatic. The only parameter that has to be chosen is the order of truncature, and this can easily be automated. Particularly, there is no need to decide *a priori* the step length as in a step-by-step procedure. The range of validity of the asymptotic-numerical solution is analysed *a posteriori* by determining the radius of convergence of the series. In fact, the range of validity, or the step length, is given by the method itself and it is not chosen *a priori* by the user.

Already now, we have shown on two plate and shell problems that the method is able to complete a linear buckling analysis in an automatic manner, and with a computing time that is rather small as compared to the linear buckling analysis. It is an effective tool for giving an insight into the postbuckling behaviour. Nevertheless, the present method would be much more attractive if the range of validity of the polynomial series could be significantly extended. It seems that the use of Padé approximants will permit us to achieve this goal, and we are currently investigating this. The reduce basis technique of Noor and Peters¹⁷ also seems to be an interesting way of completing the present analysis.

Here, we have not considered any imperfections, and the present asymptotic numerical method is only an abridged version of the original method proposed by Damiel and Potier–Ferry.⁹ Imperfection sensitivity analysis requires additional works that are carried out for imperfect cylindrical shells. In this case, a class of non-linear problems will be solved by inverting only one stiffness matrix.

Finally, we are also adapting such asymptotic-numerical procedures for the computation of any non-linear solution of a plate or a shell problem, and not only the bifurcating branches. Because it is rapid and automatic, this method could be the basis of an efficient continuation procedure.

APPENDIX

In the case where there is coupling between membrane and flexion in the constitutive equation, we have, instead of (5),

$$\mathbf{N} = \mathbf{C}_m : \boldsymbol{\Gamma} + \mathbf{C}_{mb} : \mathbf{K} \quad (42)$$

$$\mathbf{M} = \mathbf{C}_{mb} : \boldsymbol{\Gamma} + \mathbf{C}_b : \mathbf{K} \quad (43)$$

Defining the inverse of the above relation by

$$\Gamma = \mathbf{S}_m : \mathbf{N} + \mathbf{S}_{mb} : \mathbf{M}$$

$$\mathbf{K} = \mathbf{S}_{mb} : \mathbf{N} + \mathbf{S}_b : \mathbf{M}$$

equations (6)–(8), (11), (18) and (19) should be replaced by

$$\mathcal{W}(\Gamma, \mathbf{K}) = \frac{1}{2} \Gamma : \mathbf{C}_m : \Gamma + \frac{1}{2} \mathbf{K} : \mathbf{C}_b : \mathbf{K} + \Gamma : \mathbf{C}_{mb} : \mathbf{K} \quad (44)$$

$$\mathcal{W}^*(\mathbf{N}, \mathbf{M}) = \frac{1}{2} \mathbf{N} : \mathbf{S}_m : \mathbf{N} + \frac{1}{2} \mathbf{M} : \mathbf{S}_b : \mathbf{M} + \mathbf{N} : \mathbf{S}_{mb} : \mathbf{M} \quad (45)$$

$$\mathcal{L}(U_\alpha, W, \mathbf{N}) = \int_{\Omega} (\Gamma : \mathbf{N} - \frac{1}{2} \mathbf{N} : \mathbf{C}_m^{-1} : \mathbf{N}) + (\frac{1}{2} \mathbf{K} : \mathbf{C}_m^{-1} : \mathbf{K}) + (\mathbf{K} : \mathbf{C}_{mb} : \mathbf{C}_m^{-1} : \mathbf{N}) d\Omega - \lambda \mathcal{P}(U_\alpha, \mathbf{W}) \quad (46)$$

$$\begin{aligned} \langle \langle L(\mathbf{U}), \delta \mathbf{U} \rangle \rangle &= \int_{\Omega} \mathbf{N} : \delta \Gamma^L + (\Gamma^L - \mathbf{C}_m^{-1} : \mathbf{N} + \mathbf{C}_m^{-1} : \mathbf{C}_{mb} : \mathbf{K}) : \delta \mathbf{N} \\ &\quad + (\mathbf{S}_b^{-1} : \mathbf{K} + \mathbf{C}_{mb} : \mathbf{C}_m^{-1} : \mathbf{N}) : \delta \mathbf{K} d\Omega + \lambda_c \int_{\Omega} \mathbf{N}^0 : \delta \Gamma^{NL} d\Omega \end{aligned} \quad (47)$$

$$\mathbf{N}(p) = \mathbf{C}_m : (\Gamma^L(p) - \mathbf{F}^N(p)) + \mathbf{C}_{mb} : \mathbf{K}(p) \quad (48)$$

$$\begin{aligned} \langle \langle \bar{L}(\bar{\mathbf{V}}(p)), \delta \bar{\mathbf{U}} \rangle \rangle &= \int_{\Omega} (\mathbf{C}_m : \Gamma^L + \mathbf{C}_{mb} : \mathbf{K}) : \delta \Gamma^L \\ &\quad + (\mathbf{C}_{mb} : \Gamma^L + \mathbf{C}_b : \mathbf{K}) : \delta \mathbf{K} d\Omega + \lambda_c \int_{\Omega} \mathbf{N}^0 : \delta \Gamma^{NL} d\Omega \end{aligned} \quad (49)$$

$$\langle \langle \bar{\mathbf{F}}(p), \delta \bar{\mathbf{U}} \rangle \rangle = \int_{\Omega} \mathbf{F}_\alpha^U(p) \delta W_{,\alpha} + \mathbf{C}_m : \mathbf{F}^N(p) : \delta \Gamma^L + \mathbf{C}_{mb} : \mathbf{F}^N(p) : \delta \mathbf{K} d\Omega \quad (50)$$

REFERENCES

1. W. C. Rheinboldt, 'Numerical continuation methods for finite element applications', in K. J. Bathe *et al.* (eds.), *Formulation and Computational Algorithm in Finite Element Analysis*, The Massachusetts Institute of Technology, MA, 1976.
2. W. Wagner and P. Wriggers, 'A simple method for the calculation of postcritical branches', *Eng. Comput.*, **5**, 103–109 (1991).
3. R. Kouhia and M. Mikkola, 'Tracing the equilibrium path beyond simple critical points', *Int. j. numer. methods eng.*, **28**, 2923–2941 (1989).
4. E. Riks, 'An incremental approach to the solution of snapping and buckling problems', *Int. j. solids struct.*, **15**, 529–551 (1979).
5. E. Ramm, 'Strategies for tracing the nonlinear response near limit points', in *Nonlinear Finite Element Analysis in Structural Mechanics*, European U.S. Workshop, Ruhr Universität Bochum, Germany, Springer, Berlin, 1981, pp. 63–89.
6. M. A. Criesfield, 'An arc-length method including line search and acceleration', *Int. j. numer. methods eng.*, **19**, 1269–1289 (1983).
7. W. Wagner, 'A path-following algorithm with quadratic predictor', *Comput. struct.*, **39**(3/4), 339–348 (1991).
8. A. Eriksson, 'Derivatives of tangential stiffness matrices for equilibrium path descriptions', *Int. j. numer. methods eng.*, **32**, 1093–1113 (1991).
9. N. Damil and M. Potier-Ferry, 'A new method to compute perturbed bifurcations: application to the buckling of imperfect elastic structures', *Int. J. Eng. Sci.*, **28**(9), 943–957 (1990).
10. W. T. Koiter, 'On the stability of elastic equilibrium', *Thesis*, Delft, 1945; English translation NASA Techn. Trans. F. **10**, 883 (1967).
11. B. Budiansky, 'Theory of buckling and post-buckling behaviour of elastic structures', *Adv. Appl. Mech.*, **14**, 1–65 (1974).
12. M. Potier-Ferry, 'Foundations of elastic post-buckling theory', in *Buckling and Post-Buckling*, Lecture Notes in Physics, Vol. 288, Springer, Berlin, 1987, pp. 1–82.

13. D. A. Nagy and M. König, 'Geometrically nonlinear finite element behaviour using buckling mode superposition', *Comput. Methods Appl. Mech. Eng.*, **19**, 447–484 (1979).
14. J. J. Connor and N. Morin, 'Perturbation techniques in the analysis of geometrically nonlinear shells', *Proc. Symp. on High Speed Comp. of Elastic Structures*, Liege, 1970.
15. R. H. Gallagher, 'Perturbation procedures in nonlinear finite element structural analysis', *Proc. Int. Conf. on Comp. Method in Nonl. Mech.*, Austin, Texas, 1974.
16. I. W. Glaum, T. Belytschko and E. F. Masur, 'Buckling of structures with finite prebuckling deformations—a perturbation FEA', *Int. j. solids struct.*, **11**, 1023–1033 (1975).
17. A. K. Noor and J. M. Peters, 'Reduced basis technique for nonlinear analysis of structures', *AIAA J* **18**(4), 455–462 (1980).
18. A. K. Noor and C. M. Andersen, 'Hybrid analytical technique for the nonlinear analysis of curved beams', in P. Wriggers and W. Wagner (eds.), *Non-Linear Computational Mechanics—State of Art*, Springer, Berlin, 1991.
19. J. F. Bessling, 'Post-buckling and nonlinear analysis by the finite element method as a supplement to a linear analysis', *ZAAM*, **55**(4), 3–16 (1975).
20. A. C. Walker, 'A non-linear FEA of shallow circular arches', *Int. j. solids struct.*, **5**, 97–102 (1969).
21. M. Van Dyke, 'Computer-extended series', *Ann. Rev. Fluid Mech.*, **16**, 287–309 (1984).
22. N. Yamaki, *Elastic Stability of Circular Cylindrical Shells*, North-Holland, Amsterdam, 1984.
23. J. L. Batoz, K. J. Bathe and L. W. Ho, 'A study of three node triangular plate bending elements', *Int. j. numer. methods. eng.*, **15**, 1771–1812 (1980).
24. ● C. Zienkiewicz, *The Finite Element Method*, 3rd edn., Mc-Graw-Hill, London, 1977.
25. D. H. Sattinger, 'Transformation groups and bifurcation at multiple eigenvalues', *Bull. Am. Math. Soc.* **79**(4), (1973).
26. G. A. Baker and P. Graves-Morris, *Padé Approximants, Part I: Basic Theory. Encyclopedia of Mathematics and its Applications*, Vol. 13, Addison-Wesley, Reading, MA, 1981.